Aeroelastic Analysis of an Aircraft Wing Structure – the Use of a Discrete-Time Model

Uthit Inthachub[1*], **Sujin Bureerat**[2]

Department of Mechanical Engineering, Faculty of Engineering, Khon Kaen University, Khon Kaen 40002, Thailand
Tel: 0-4320-2845, Fax: 0-4320-2849, *E-mail: uthiteng@yahoo.com[1*], sujbur@kku.ac.th[2]

Abstract

Aeroelasticity describes the phenomena of an aircraft structural system when the mutual interaction between inertial, restoration and aerodynamic forces takes place. It is one of the most important criteria in aircraft structural design. This work is concerned with the development of program codes for aeroelastic analysis of an aircraft structure. A discrete-time aeroelastic model and flutter analysis are detailed. Structural dynamic analysis is achieved by using the finite element method while aerodynamic and aeroelastic computations are carried out using the MATLAB program codes. A wing box structure made of aluminium is chosen for the demonstration of aeroelastic design and analysis. It is illustrated that the MATLAB program developed can be used as a tool for analysis and design of aircraft wings and tails.

Keywords: Discrete-Time Aeroelastic Model, Flutter Analysis, Aerodynamics, Vortex Ring Method

1. Introduction

In the part, classical aircraft design simply minimised the elastic structural defections of a large and stiff lifting-surface structure so as to reduce undesirable aeroelastic phenomena. Later, with the development of multidisciplinary design optimisation (MDO) technology, the use of elastic deflections to enhance the aerodynamic performance of practical structures has become possible. Weight and size reductions and performance improvement can be expected by using the advantages of structural flexibility. The development of advanced computational aeroelasticity and smart material enables the new direction of aircraft structure. It is the concept of mimicking a bird wing so that an aircraft can have a multi-role flight. With such idea, the wing can be highly flexible; therefore, the subject of aeroelasticity is even more important for aircraft structural design.

This paper presents the progress on aeroelastic research work conducted at Khon Kaen University. A discrete-time aeroelastic model and flutter analysis are detailed. Structural dynamic analysis is achieved by using the finite element method while aerodynamic and aeroelastic computations are carried out using the MATLAB panel codes. A wing-box structure made of aluminium is chosen for aeroelastic analysis demonstration. It can be concluded that the developed program can be used as a tool for aircraft design research in the future.

2. Theory

Discrete-time aeroelastic model in this work is similar to the techniques presented in [1] and [2] with some modification and corrections. Most of the variables used in this paper are taken from [2]. Figure 1 shows a typical wing-box structure consisting of 2 spars and 2 ribs with upper & lower skins. The finite element grid of the structure is displayed in Figure 2. For aerodynamic analysis using the vortex ring method [3], the wing is represented by the surface of the wing's chambers which is called a lifting-surface. Aerodynamic analysis of the wing's lifting-surface is advantageous in that it is simple to calculate, needs less computational time, and provides acceptable computation results. The aerodynamic model is shown in Figure 3.

When the structure is subjected to aerodynamic loads, it is deformed resulting in the change of the aerodynamic lifting-surface configuration. With this lifting-surface being distorted, the aerodynamic characteristics of the wing are simultaneously altered. This phenomenon is called fluid/structure interaction. Structural inertia takes part when the structure is in motion. Much work has been made towards aeroelastic analysis and design e.g. in [3] and [4]. One of the most important aeroelastic phenomena that are used in aircraft design is flutter analysis. The word flutter is usually referred to as a critical wind speed that causes dynamic instability of a structure. One of the most popular flutter analysis techniques is the use of the doublet lattice method in combination with finite element analysis where the flutter speed is solved on the frequency domain. This can be found in MSC/NASTRAN or MBB-LaGrange commercial software. The other well-known approach is used in the software ZAERO. The objective of developing the discrete-time aeroelastic model in this paper is to provide the more versatile aeroelastic tool that can be implemented on a variety of aircraft design applications.

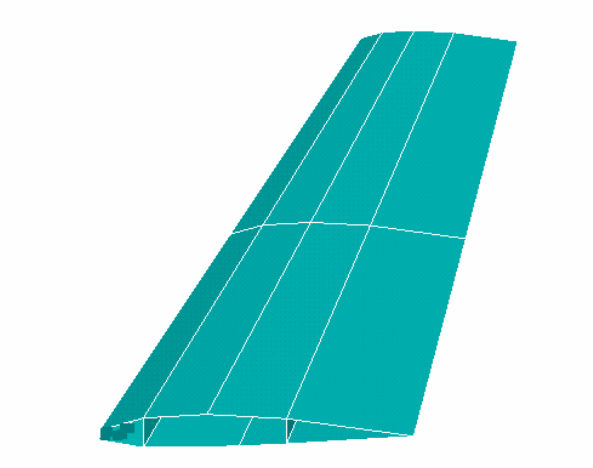

Figure 1 Wing box

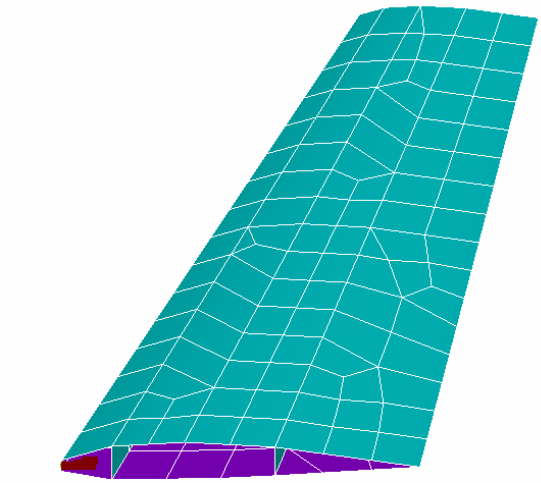

Figure 2 FEM grid of a wing

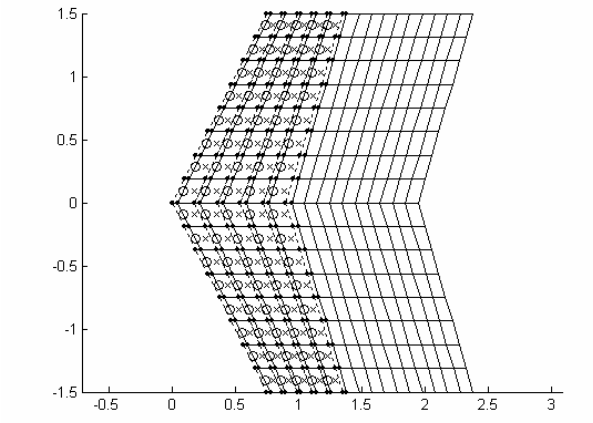

Figure 3 Aerodynamic grid

2.1 Structural model

Structural dynamic model can be described as a structure being in the state of dynamic equilibrium. It is the state at which the system having minimum potential energy (including the work due to inertial forces, external forces and system restorations). The equations of motion basically comprise of kinetic energy, structural restoration (spring and damping) and external dynamic forces. By using the finite element approach, a structural model can be written as

$$\mathbf{M}\ddot{\mathbf{u}} + \mathbf{C}\dot{\mathbf{u}} + \mathbf{K}\mathbf{u} = \mathbf{F}_e \quad (1)$$

Where $\mathbf{M}$ = mass matrix
$\mathbf{C}$ = damping matrix (here is proportional damping)
$\mathbf{K}$ = stiffness matrix
$\mathbf{F}_e$ = nodal force vector
$\mathbf{U}$ = nodal displacement vector

The finite element model of an aircraft structure normally usually contains a large amount of degree of freedom. As a result, the size of the mass, modal damping and stiffness matrices are considerably large. Solving the system of differential equations (1) directly would be computationally expensive. Such a difficulty can however be dealt with by using a modal approach. For an N d.o.f. system, let $[\Phi] = [\{\vec{\mathbf{u}}\}_1, \{\vec{\mathbf{u}}\}_2, ..., \{\vec{\mathbf{u}}\}_M]$ be the matrix of M selected eigenvectors of the free vibration problem

$$\mathbf{K} - \lambda\mathbf{M} = \mathbf{0} \quad (2)$$

where $M << N$. The modal coordinates can be defined as

$$\mathbf{u} = [\Phi]\mathbf{x} \quad (3)$$

Substituting (3) to (1) and pre-multiplying (1) by $[\Phi]^T$ lead to the reduced-order structural model

$$\mathbf{M}_g\ddot{\mathbf{x}} + \mathbf{C}_g\dot{\mathbf{x}} + \mathbf{K}_g\mathbf{x} = \mathbf{F}_g \quad (4)$$

where

$$\mathbf{M}_g = [\Phi]^T\mathbf{M}[\Phi], \mathbf{C}_g = [\Phi]^T\mathbf{C}[\Phi],$$
$$\mathbf{K}_g = [\Phi]^T\mathbf{K}[\Phi], \mathbf{F}_g = [\Phi]^T\mathbf{F}_e$$

Equation (4) can be transformed to be a continuous-time state-space model as

$$\begin{bmatrix}\mathbf{M}_g & \mathbf{C}_g \\ \mathbf{0} & \mathbf{M}_g\end{bmatrix}\begin{Bmatrix}\ddot{\mathbf{x}} \\ \dot{\mathbf{x}}\end{Bmatrix} + \begin{bmatrix}\mathbf{0} & \mathbf{K}_g \\ -\mathbf{M}_g & \mathbf{0}\end{bmatrix}\begin{Bmatrix}\dot{\mathbf{x}} \\ \mathbf{x}\end{Bmatrix} - \begin{Bmatrix}\mathbf{F}_g \\ \mathbf{0}\end{Bmatrix} = \mathbf{0} \quad (5)$$

or

$$\mathbf{A}_c\dot{\mathbf{q}} + \mathbf{B}_c\mathbf{q} - \mathbf{F}_c = \mathbf{0} \quad (6)$$

where the vector of state variables is

$$\mathbf{q} = \begin{bmatrix}\dot{\mathbf{x}} \\ \mathbf{x}\end{bmatrix}.$$

The state-space equation (5) can be converted to its discrete-time counterpart by substituting

$$\mathbf{q} = \frac{\mathbf{q}^{n+1} + \mathbf{q}^n}{2}, \dot{\mathbf{q}} = \frac{\mathbf{q}^{n+1} - \mathbf{q}^n}{\Delta t} \quad (7)$$

to equation (5) leading to

$$[DEOM_2]\mathbf{q}^{n+1} + [DEOM_1]\mathbf{q}^n + \mathbf{F}^{n+1/2} = \mathbf{0} \quad (8)$$

where

$$[DEOM_2]=\begin{bmatrix}\frac{1}{\Delta t}\mathbf{M}_g & \frac{1}{\Delta t}\mathbf{C}_g+\frac{1}{2}\mathbf{K}_g\\ -\frac{1}{2}\mathbf{M}_g & \frac{1}{\Delta t}\mathbf{M}_g\end{bmatrix},$$

$$[DEOM_1]=\begin{bmatrix}-\frac{1}{\Delta t}\mathbf{M}_g & -\frac{1}{\Delta t}\mathbf{C}_g+\frac{1}{2}\mathbf{K}_g\\ -\frac{1}{2}\mathbf{M}_g & -\frac{1}{\Delta t}\mathbf{M}_g\end{bmatrix}$$

$$\mathbf{F}^{n+1/2}=\begin{bmatrix}-\mathbf{F}_g\\ \mathbf{0}\end{bmatrix}$$

Cleary, the discrete-time structural model is proposed so that the discrete-time aerodynamics can be employed and it is also useful when active aeroelastic design is involved.

2.2 Aerodynamic model

The discrete time unsteady vortex ring method detailed in [5] is used for aerodynamic analysis. The method is based upon the potential flow analysis where the wing is represented by its lifting-surface. Having discretised the lifting-surface and wake vortex and with the use of Biot-Sawart law, the aerodynamics at the time step *n* can be written in algebraic form as

$$[AIC]\boldsymbol{\Gamma}^n=\mathbf{W}^n \tag{9}$$

where [*AIC*] = aerodynamic influence coefficient matrix

$\boldsymbol{\Gamma}^n$ = the vector of vortex ring strength at the time step *n*

$\mathbf{W}^n$ = the vector of the downwash at the collocation points at the time step *n*.

Adding the unsteady conditions of wake vortices to (9), the discrete-time aerodynamic model is of the from (see [1] and [2] for more details)

$$[CDR_2]\boldsymbol{\Gamma}^{n+1}+[CDR_1]\boldsymbol{\Gamma}^n=\mathbf{W}^n \tag{10}$$

The pressure acting upon each panel of the lifting-surface is determined by using the unsteady Bernoulli's equation leading to

$$\Delta\mathbf{P}^{n+1/2}=\rho\left[U\frac{\Gamma_{i,j}-\Gamma_{i-1,j}}{\Delta c_{i,j}}+\frac{d\Gamma_{i,j}}{dt}\right] \tag{11}$$

which can be written in the discrete from as

$$\Delta\mathbf{P}^{n+1/2}=\rho U\left[\frac{\Gamma_{i,j}^{n+1}+\Gamma_{i,j}^{n}-\Gamma_{i-1,j}^{n+1}-\Gamma_{i-1,j}^{n}}{2\Delta c_{i,j}}+\frac{\Gamma_{i,j}^{n+1}-\Gamma_{i,j}^{n}}{\Delta x}\right] \tag{12}$$

For more details, see reference [5]. After some rearrangements and manipulations, equation (12) can be expressed as

$$\Delta\mathbf{P}^{n+1/2}=[C2P_2]\boldsymbol{\Gamma}^{n+1}+[C2P_1]\boldsymbol{\Gamma}^n \tag{13}$$

2.3 Interfacing aerodynamic forces to a structural model

Since the aerodynamic and structure models are obtained from the different approaches, the sets of aerodynamic panels and structure elements are usually incompatible to each other. Matching them together can be carried out by using surface spline interpolation [6]. Let $\mathbf{u}_A$ be the displacements at the vortex points corresponding to the panel forces. With the use of the interpolation technique, the relationship between the displacements of structural nodal points and the displacements of the vortex points can be approximated as

$$\mathbf{u}_A=[G]\mathbf{u} \tag{14}$$

where [*G*] is a transformation matrix. The external force vector in (1), which can be seen as the work done by external loads or the product of $\mathbf{F}_A$ and $\mathbf{u}_A$, can be obtained as the following equation

$$\mathbf{F}_e=[G]^T\mathbf{F}_A \tag{15}$$

Similarly to (14), the downwash vector due to structural deformation can be written as

$$\mathbf{W}^n=U_\infty[H]\mathbf{u} \tag{16}$$

where [*H*] is a transformation matrix obtained from using the interpolation technique, and U_∞ is a wind speed. Equation (16) can be rearranged leading to

$$\mathbf{W}^n=U_\infty[H][\Phi]\mathbf{T}_0\mathbf{q}^n$$

or

$$\mathbf{W}^n=[WDR]\mathbf{q}^n \tag{18}$$

The pressure difference at the wing panel surface is transformed to be structural nodal forces using the relation

$$\mathbf{F}_A^{n+1/2}=[S]\Delta\mathbf{P}^{n+1/2} \tag{19}$$

where [*S*] is the surface area of the panels.

Solving (13), (15) and (19) and using the definition of $\mathbf{F}_g$ in (4), one can obtain

$$\begin{aligned}\mathbf{F}_g&=[\Phi]^T[G]^T[S][C2P_2]\boldsymbol{\Gamma}^{n+1}\\&+[\Phi]^T[G]^T[S][C2P_1]\boldsymbol{\Gamma}^n\\&=[C2F_2]\boldsymbol{\Gamma}^{n+1}+[C2F_1]\boldsymbol{\Gamma}^n\end{aligned} \tag{20}$$

From (8),

$$\mathbf{F}^{n+1/2}=\begin{bmatrix}-\mathbf{F}_g\\ \mathbf{0}\end{bmatrix}=\begin{bmatrix}-[\Phi]^T[G]^T[S]\Delta\mathbf{P}^{n+1/2}\\ \mathbf{0}\end{bmatrix} \tag{21}$$

or

$$\mathbf{F}^{n+1/2}=[CNFR_2]\boldsymbol{\Gamma}^{n+1}+[CNFR_1]\boldsymbol{\Gamma}^n \tag{22}$$

where

$$[CNFR_2]=\begin{bmatrix}-[C2F_2]\\ \mathbf{0}\end{bmatrix}\text{ and }[CNFR_1]=\begin{bmatrix}-[C2F_1]\\ \mathbf{0}\end{bmatrix}.$$

2.4 Flutter analysis

Flutter is the dynamic instability of an aircraft wing structure consisting of a violent unstable oscillation. During flight, the dynamic characteristics change with airspeed and altitude. At some speed, the structural

modes will interact in such a way that motion becomes unstable. The critical speed at which the instability occurs is called the flutter speed. The accuracy of the aeroelastic stability analysis was investigated by avoiding undesirable flutter phenomena.

A discrete-time aeroelastic mathematical model is composed of four basic parts [2].

- Circulation-downwash relation from the vortex ring method (10)
- Wing motion – downwash relation (18)
- Discrete time equation of motion from the finite element formulation (8)
- Circulation-nodal force relation from the unsteady Bernoulli equation and work equivalent load method (22)

From equations (10) and (18), one can have

$$[CDR_2]\boldsymbol{\Gamma}^{n+1} + [CDR_1]\boldsymbol{\Gamma}^{n} - [WDR]\mathbf{q}^{n} = \mathbf{0} \qquad (23)$$

Combining (8) and (22) leads to

$$[CNFR_2]\boldsymbol{\Gamma}^{n+1} + [CNFR_1]\boldsymbol{\Gamma}^{n} + [DEOM_2]\mathbf{q}^{n+1} + [DEOM_1]\mathbf{q}^{n} = \mathbf{0} \qquad (24)$$

Finally the complete discrete-time state space equation is of the form

$$\begin{bmatrix} [CDR_2] & -[WDR] \\ [CNFR_2] & [DEOM_2] \end{bmatrix} \begin{bmatrix} \boldsymbol{\Gamma} \\ \mathbf{q} \end{bmatrix}^{n+1} + \begin{bmatrix} [CDR_1] & [0] \\ [CNFR_1] & [DEOM_1] \end{bmatrix} \begin{bmatrix} \boldsymbol{\Gamma} \\ \mathbf{q} \end{bmatrix}^{n} = \mathbf{0} \qquad (25)$$

A flutter speed can be achieved by solving the discrete-time eigenvalue problem (25) at various wind speeds. At a particular wind speed, equation (25) is obtained and the eigenvalue problem is solved. The discrete-time eigenvalues can be altered to be their continuous-time counterparts by taking the natural logarithm and dividing by the time interval Δt. The speed at which one of the real parts of the continuous-time eigenvalues becomes greater than zero is taken as the flutter speed. The use of a reduced-order model is said to be more efficient than the full model in terms of computational time [1] but the work in this paper will present only the full model.

3. Numerical Test

A numerical experiment is made to somewhat verify the program codes. A simple wing structure without control surfaces is used for the numerical test, and it is displayed in Figure 1. The wing consists of 2 ribs and 2 spars with upper and lower skins. Figure 4 shows the assembly of ribs and spars of the wing. The wing cross-section is proportional to the NACA4212 airfoil section shown in Figure 5. The dimensions of the wing are given in Figure 6 where the semi-span length L = 1.5 m, the root chord RC = 0.6 m, the tip chord TC = 0.3 m, and the swept angle Λ = 30°. The structure is made of aluminium with the Young's modulus of 70 x 10^9 N/m^2, the Poisson ratio of 0.34 and the density of 2700 kg/m^3. The skin thickness of the wing box is 2 mm whereas the thickness of the ribs and spars are 3 mm.

Two cases of analysis are studied here, the first case is the study of the effect of panel box numbers and the second study is the effect of wake length on the computational results. Given that N_{ch} is the number of vortex ring grids in the chordwise direction, N_{sp} is the number of vortex ring grids in the spanwise direction, and N_{wk} is the number of wake grids in the streamwise direction. Thus, the total number of vortex rings is $N_{ch}\times N_{sp} + N_{wk}\times N_{sp}$ for a symmetrical lifting-surface. Note that a particular unsteady aerodynamic model termed $N_{ch}\times N_{sp}\times N_{wk}$ means the model using $N_{ch}\times N_{sp}$ wing panels and $N_{sp}\times N_{wk}$ wake panels. For the first studying case, the aerodynamics models are detailed in Table 1 while the aerodynamic models for the second studying case are detailed in Table 2.

Table 1 Aerodynamic models for case 1

Model	$N_{ch}\times N_{sp}\times N_{wk}$
1	5×8×25
2	6×9×25
3	7×10×25
4	8×11×25

Table 2 Aerodynamic models for case 2

Model	$N_{ch}\times N_{sp}\times N_{wk}$
1	5×8×10
2	5×8×15
3	5×8×20
4	5×8×25

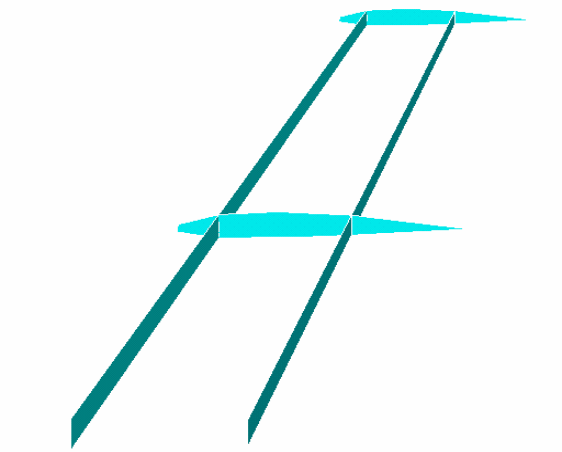

Figure 4 Wing ribs and spars

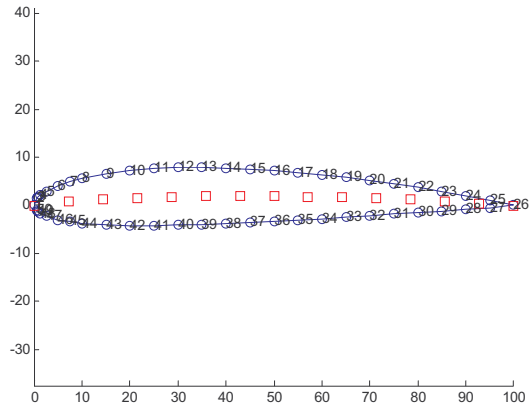

Figure 5 NACA4212 airfoil section

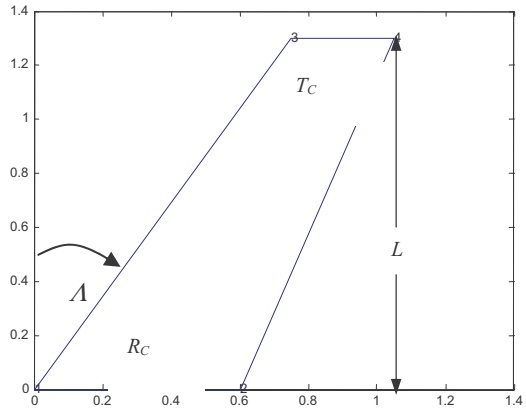

Figure 6 Wing dimensions

4. Numerical Results

The structural modal analysis results of the wing are given in Table 3 where the first 5 fundamental modes are selected for aeroelastic calculation. The mode shapes of the wing are illustrated in Figures 7-11.

Table 3 Wing natural frequencies

Mode no.	Natural frequency
1	30.73
2	127.07
3	167.18
4	183.82
5	199.67

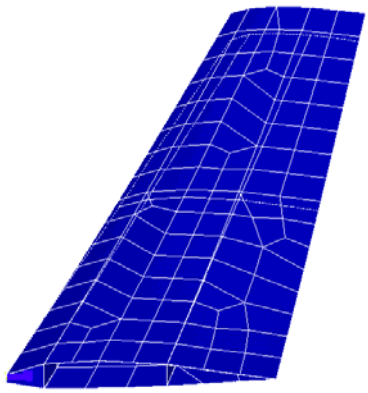

Figure 7 First Mode shape

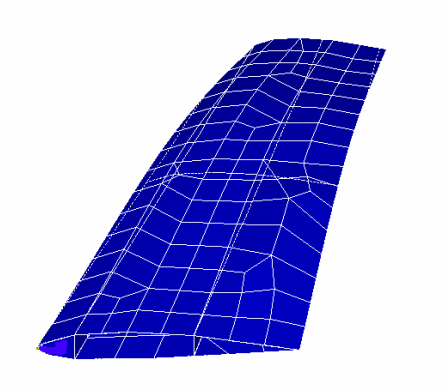

Figure 8 Second Mode shape

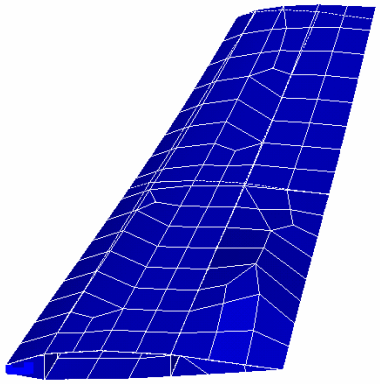

Figure 9 Third Mode shape

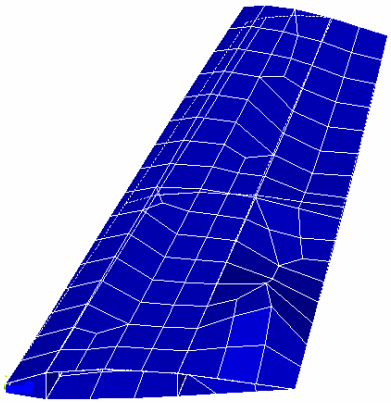

Figure 10 Fourth Mode shape

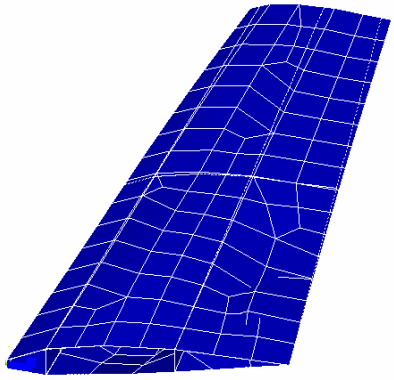

Figure 11 Fifth Mode shape

Figure 12 displays the plot of discrete-time eigenvalues of the first model of case 1. The eigenvalues of the second model are plotted in Figure 13, and the eigenvalues of the third and fourth models are plotted in Figures 14 and 15 respectively. All the plots have 25 branches equal to N_{wk}. The number of circles inside the branches is normally equal to N_{sp}. It however needs some careful observation to see all of them. The plot of the discrete-time eigenvalues of the second, third and fourth models of case 2 are displayed in Figures 16, 17 and 18 respectively. Similarly to the first studying case, the number of branches is equal to N_{wk} while the number of inside rings, which is quite difficult to identify from merely observing, is equal to N_{sp}.

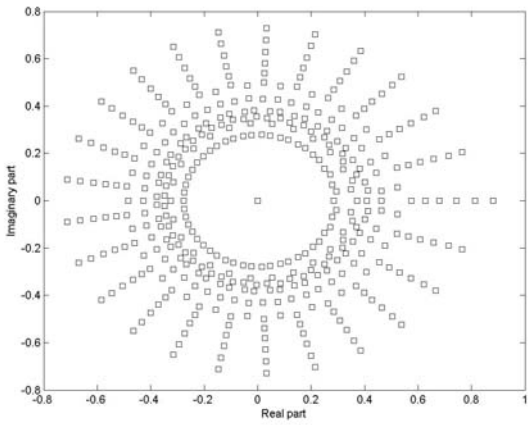

Figure 12 Discrete time eigenvalues of the 5×8×25 aerodynamic model

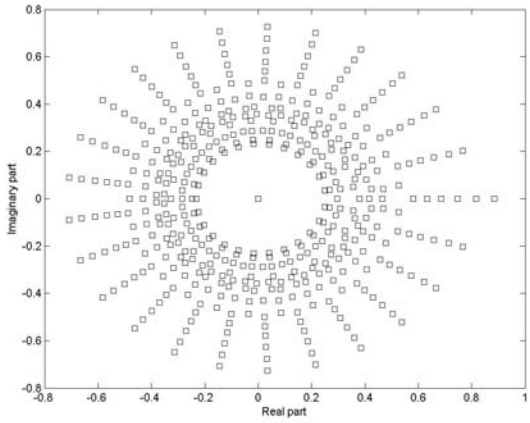

Figure 13 Discrete time eigenvalues of the 6×9×25 aerodynamic model

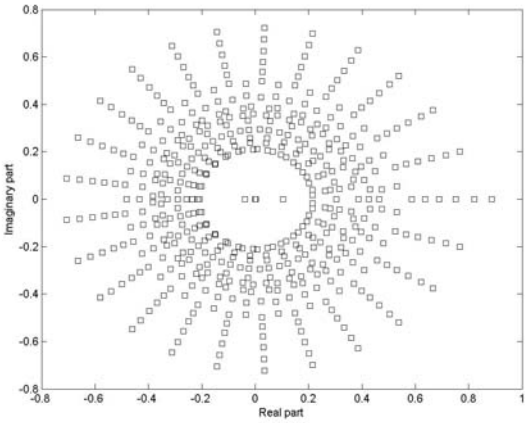

Figure 14 Discrete time eigenvalues of the 7×10×25 aerodynamic model

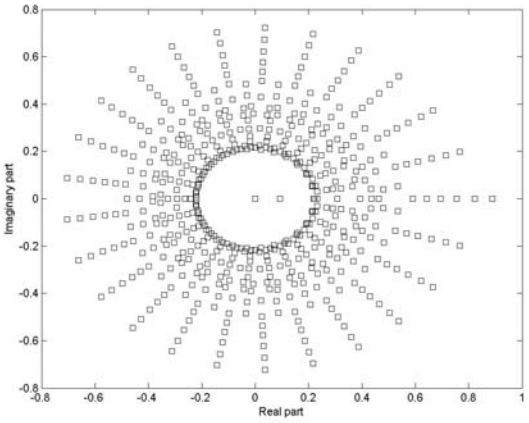

Figure 15 Discrete time eigenvalues of the 8×11×25 aerodynamic model

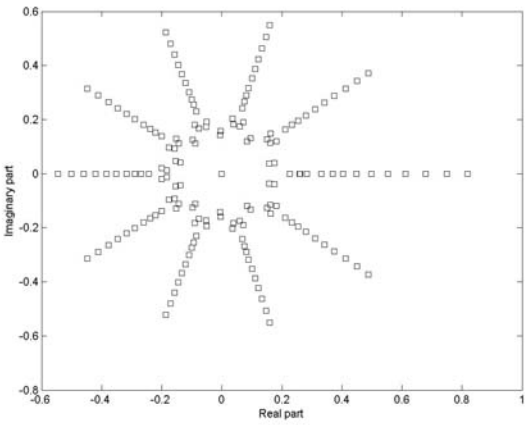

Figure 16 Discrete time eigenvalues of the 5×8×10 aerodynamic model

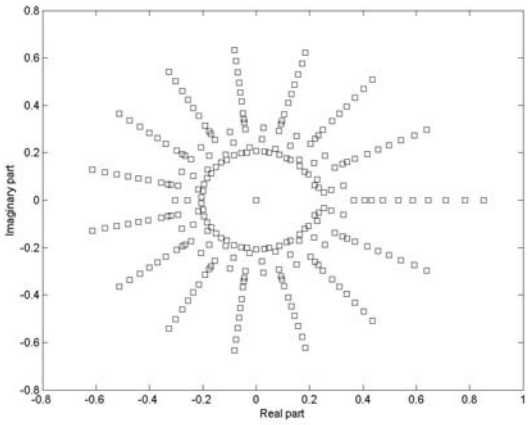

Figure 17 Discrete time eigenvalues of the 5×8×15 aerodynamic model

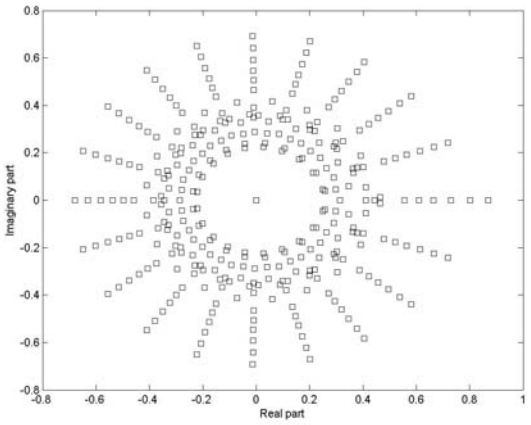

Figure 18 Discrete time eigenvalues of the 5×8×20 aerodynamic model

The 5×8×25 aerodynamic model is chosen to illustrate the flutter analysis. The plot of real and imaginary parts of the continuous-time eigenvalues against the various velocities is given in Figure 19. Figure 20 shows the magnified version of Figure 19. It is shown that the wing begins unstable at the speed of 80 m/s approximately. The time history of the modal displacements (**q**) of the wing at U_∞ = 20 m/s is shown in Figure 21 where the initial conditions are given. It can be seen that the state variables are converged after a perturbation. The time history of the wing displacement at U_∞ = 50 m/s is displayed in Figure 22. It is shown that the system converges to the stable points slower than when the wind speed is 20 m/s. In Figure 23, the time history of the displacements at U_∞ = 90 m/s, which is in the unstable boundary is depicted. It can be seen that the displacements are diverged as the time goes on. This somewhat indicates that the results in the time domain are corresponding to those in the frequency domain. The other computed flutter speeds using the various aerodynamic models are given in table 4. It should be noted that the obtained results are from observing the plot in MATLAB figures.

Table 4 Flutter speeds from the various aerodynamic models

Case	Model	Flutter speed m/s
1	1	80
	2	110
	3	80
	4	60
2	1	80
	2	80
	3	80
	4	80

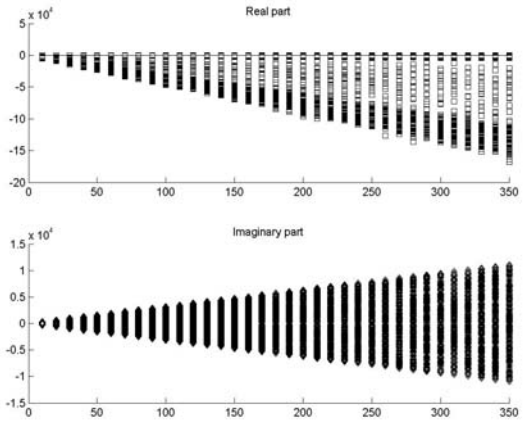

Figure 19 Real and imaginary parts of eigenvalues versus wind velocity: the 5×8×25 aerodynamic model

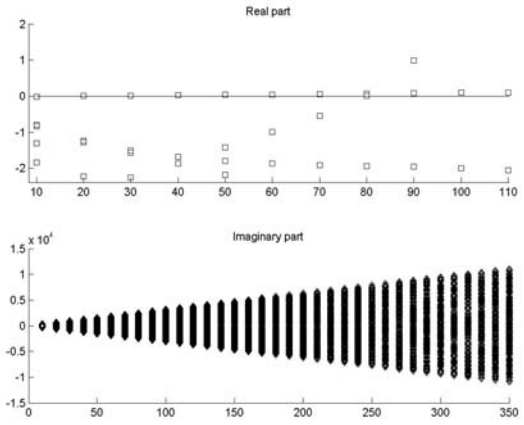

Figure 20 Magnification of Figure 19

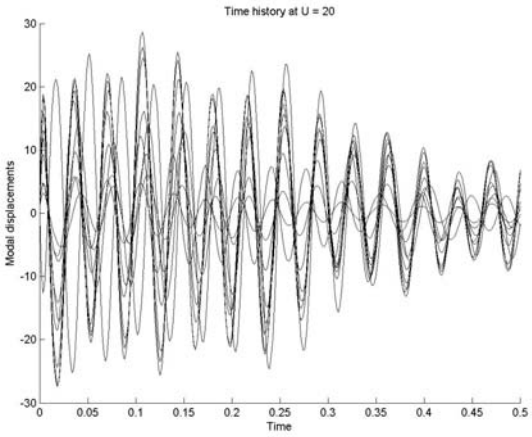

Figure 21 Time history of the modal coordinates at U_∞ = 20 m/s

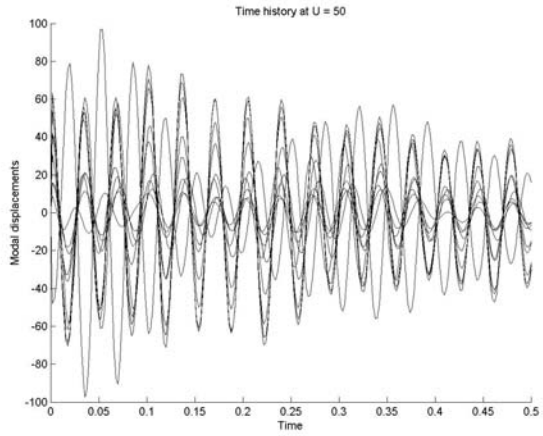

Figure 22 Time history of the modal coordinates at U_∞ = 50 m/s

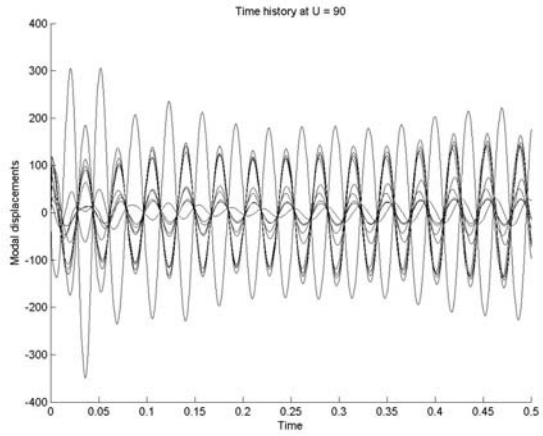

Figure 23 Time history of the modal coordinates at U_∞ = 90 m/s

5. Conclusions, Discussion and Future Work

The discrete-time aerodynamic and aeroelastic models are briefly detailed. The effects of panel number on the analysis results are studied. The numerical results are obtained, illustrated and discussed.

The future work will be the use of a reduced-order aerodynamic model to save computing time. Also, the development of the mode tracking systems has to be carried out. It has been found that the classical methods like modal assurance criterion (MAC) [7] and eigenvalue derivative [8] and [9] cannot be applied successfully. The other part is static aeroelasticity which includes lift and control effectiveness, control reversal, and divergence. The program codes will be further developed particularly in the part of finite element analysis and optimisation. This approach when perfectly developed is expected to be used for design and synthesis of a morphing aircraft wing as well as active aeroelastic control of a real-world aircraft structure.

Acknowledgments

The authors are grateful for the financial support from Sustainable Infrastructure Research and Development Center (SIRDC) and faculty of engineering, Khon Kaen University.

References

[1] Kenneth C. Hall., 1994. Eigenanalysis of Unsteady Flows About Airfoils, Cascades, and Wings. AIAA, Vol.32 No.12, pp. 2426-2432

[2] Hak-Tae Lee, Ilan M.Kroo, and Stefan Bieniawski., 2002. Flutter Suppression for High Aspect Ratio Flexible Wings Using Microflaps. AIAA2002-1717, April 22-25, pp.1-10

[3] Pendleton E., 2000. Back to the Future How Active Aeroelastic Wings are a Return to Aviation's Beginnings and a Small Step to Future Bird-like Wings. RTO-SMP Panel Meeting.

[4] Flick P. and Love M., 1999. The Impact of Active Aeroelastic Wing Technology on Conceptual Aircraft Design. AVT Panel Meeting. Ottawa.

[5] Katz, J., Plotkin. A,. LOW-SPEED AERODYNAMIC: from wing theory to panel methods, Mcgraw-Hill, Singapore, 1991.

[6] Robert L. Harder, Robert N. Desmarais,1971. Interpolation Using Surface Splines. J. AIRCRAFT, Vol. 9, No. 2, pp. 189-191.

[7] Desforges M.J., Cooper J.E. and Wright J.R., 1996. Mode Tracking During Flutter Testing Using the Modal Assurance Criterion. IMechE, Vol. 210, pp. 27-37.

[8] Fox R.L. and Kapoor M.P., 1968. Rate of Change of Eigenvalues and Eigenvectors. AIAA, Vol. 6, pp. 2426-2492.

[9] ZAERO Theoretical Manual – Version 3.2.